Optical and Quantum Electronics (2022) 54:416
https://doi.org/10.1007/s11082-022-03798-2

Perfect selective metamaterial absorber with thin-film of GaAs layer in the visible region for solar cell applications

Raj Kumar[1] · Bipin K. Singh[2] · Rajesh K. Tiwari[3] · Praveen C. Pandey[1]

Received: 24 May 2021 / Accepted: 30 April 2022 / Published online: 7 June 2022

Abstract

In this paper, we have presented a new design of a metamaterial perfect absorber (MPA) consisting of three layers of metal-dielectric-metal in which the top layer is considered of special kind square patches at different places in a unit cell. This MPA exhibits wideband, wide-angle, and polarization-independent absorption performance in the visible region. The proposed MPA structure is composed of a resonator of metal and spacer of a dielectric layer. The interactions between the resonator and the coupling of metal-dielectric create the plasmonics effects which are responsible for the perfect absorption. Under a specific condition, this simulated absorber structure exhibits an extremely high broadband absorption between 591.54 and 704.40 nm wavelength range with near-unity absorption, and a single peak observed at 385.33 nm with the absorption of 94.16%. We extracted the impedance of the absorber and matched it with free space, and also demonstrated the effective permittivity and permeability. Moreover, the parametric study of the resonators, dielectric layer, and multi-band topology has also been investigated. The polarization-insensitive-based metamaterial may be utilized to improve the efficiency of different devices in the visible range. Furthermore, we have calculated the absorption of the proposed MPA under solar radiation (AM1.5) for different structural parameters. The proposed absorber greatly enhances the conversion efficiency which is highly useful for solar cells. We also determined the short circuit current density of this absorber for different thicknesses of the GaAs layer. The meta-surface of Al metal provides a good performance in comparison to other costly metals and the proposed structure may be used for different devices.

Keywords Metamaterial · Plasmonics · Perfect absorber · Impedance

✉ Praveen C. Pandey
pcpandey.app@iitbhu.ac.in

[1] Department of Physics, Indian Institute of Technology (BHU), Varanasi, U.P. 221005, India

[2] Department of Physics, University of Mumbai, Mumbai 400098, India

[3] Department of Applied Science and Humanities, ABES Engineering College, Ghaziabad 201009, India

1 Introduction

Utilizing solar radiations mainly in the visible region requires the perfect absorption of light for many energy fields include optical sensing, hot-electron devices, and solar cells. In recent years, metamaterials have attracted considerable attraction because they are dramatically manipulating and absorbing the incident electromagnetic waves. The exotic and exciting optical properties of the metamaterial have motivated researchers to focus on the different applications using such materials. Metamaterials are artificial materials with a sub-wavelength metal-dielectric structure. The physical properties like effective permittivity $\varepsilon(\omega)$, permeability $\mu(\omega)$ and refractive index (n) of these materials are assumed negative values (Smith et al. 2000; Shalaev et al. 2005). Metamaterials have been used across various frequency regions such as gigahertz, terahertz, and optical for many purposes such as antenna (Hasan et al. 2019), detector (Shoshi et al. 2015), sensors (Melik et al. 2009; Ding et al. 2015), energy harvesting (Cheng and Du, 2019), and perfect absorbers (Gao et al. 2020; Kumar et al. 2020). Perfect absorption of a specific range of EM radiation is a very important property of the metamaterials for applications such as micro-bolometers (Maier and Brueckl, 2010), sensors (Liu et al. 2010), imaging (Mahmud et al. 2017), and solar energy harvesting (Dayal and Ramakrishna, 2013, Almoneef and Ramahi, 2015). Perfect absorption can be realized when the frequency-dependent effective impedance of the metamaterial absorber becomes the same as the impedance of free space so that the reflected and transmitted waves reduce to zero (Mahmud et al. 2020). These properties are utilized to obtain electrical energy from electromagnetic energy in thermo-photovoltaic devices such as absorber, emitter (Wu et al. 2012), and photodiode, etc. It has also been observed that solar radiation can be captured by the metamaterial to improve the efficiency of photovoltaic devices. Mostly the energy of solar radiation cover ranges between 390 to 700 nm (Boriskina et al. 2013). Therefore, we need a high absorption in the range of 390 nm to 700 nm solar radiation for efficient solar cells, which can be easily achieved by suitable MPA. Ultra-thin broadband superabsorbers have also been theoretically and experimentally proposed for different applications (Ding et al. 2014; Yin et al. 2015a, b).

The first metamaterial perfect absorber was proposed in 2008 (Landy et al. 2009). This metamaterial structure consists of two plates of metal and a ring resonator with supplies the electric coupling. Most of the researchers have focused on a terahertz frequency region. Recently, reported metamaterial perfect absorber designs have provided the single-band (Mulla and Sabah 2015; Rufangura et al. 2016a, b), dual-band (Rufangura and Sabah 2015; Mulla and Sabah 2016), multi-band absorbers to improve the energy harvesting in the solar cell (Rufangura et al. 2016a, b, 2017). In the high-frequency region, multi-band metamaterial absorbers mainly provide the perfect absorption by using multiple layers. Some researchers (Dayal and Ramakrishna 2013; He et al. 2015) have been reported the metamaterial absorbers, which consist of three layers in the form of metal-dielectric-metal. They have reported multiple absorption bands in the visible and infrared regions for different unit cell structure engineering. Different metamaterial absorbers have been presented for solar energy harvesting using simplified and compact structures with highly efficient broadband, polarization-independent, and wide-angle absorptions. The published papers (Mehrabi et al. 2018; Li et al. 2019) have been demonstrated the broadband visible metamaterial absorbers with a compact and low-profile design for emitter and energy harvesting applications. Nevertheless, MPA structural engineering still needs to optimize and simplify to undertake electromagnetic energy harvesting by developing more efficient absorbers.

Solar energy is the most abundant and cleanest renewable energy source that can be captured and converted into thermal and electrical energy. Earth's surface gets a different amount of energy for different types of radiations and incident angles (Khan et al. 2018a, b). Visible radiations are playing a crucial role in solar cell applications and offer a maximum current in output. The conversion efficiency is reduced by any loss of light for solar cells. Its loss can be reduced by tiny transmission from the bottom metallic layer and minimum reflection with the help of metallic metasurface which improved the performance of solar cells. Some researchers carefully designed the absorbers to absorb some photons of visible regions with costly metals and had a low absorption efficiency (71%) that not be useful for solar cell applications (Aydin et al. 2011). Besides these features, the short circuit current density (J_{sc}) is the actual property to investigate the solar cell device. We required the high J_{sc} for potential applications with cheaper metals to reduce the cost of the device (Wang et al. 2015).

In this paper, we have introduced a new design of MPA for highly efficient solar energy absorption. The proposed MPA is composed of a metal-dielectric-metal nanostructure. The proposed absorber provides nearly perfect absorption in the visible region from wavelengths 375 nm to 750 nm using aluminum metal resonators on the gallium arsenide dielectric spacer layer and represents the 80.74% average absorption. The characteristics of the MPA have been investigated for different geometric parameters of the structures and resonators and spacer materials. Moreover, we have also investigated the effect of polarization and incident angles on the absorptions of the proposed structure. The conversion efficiency was significantly improved by the large value of $A_{AM1.5}$ under the AM1.5 solar spectrum of the solar cell. We obtained the short circuit density ($J_{sc} = 20.33$ mA/cm^2) under the AM1.5 solar illuminations and it has a great potential for solar cell applications.

2 Design and simulation

The proposed absorber structure is composed of three basic layers such as a bottom metallic layer of thickness '*h*', a dielectric spacer layer of thickness '*t*', and metallic patch resonators of thickness 'h_1'. The proposed MPA design and geometric parameters are shown in Fig. 1, and the value of each parameter is tabulated in Table 1. The periodicity of the unit cell '*p*' is liable for the resonance condition at different frequencies. The structure has two parts of metal layers which are Al (Aluminium) as the resonators and GaAs (Gallium arsenide) as a dielectric spacer layer. We have selected the aluminum metal because it is inexpensive and has less production cost as compared to the other metals (gold, silver, and copper) for the design of different types of metamaterial absorber structures (Rakic et al. 1998). In several published papers (Khan et al. 2018a, b; Mehrabi et al. 2018; Mulla et al. 2017; Mulla and Sabah 2016; Liu et al. 2015), the researchers have utilized Al metal to design the different metamaterial absorber structures and investigated their behaviors in the ultra-violet, visible and near-infrared regions, respectively. We have used CST microwave studio simulation software to simulate the proposed metamaterial absorber structure. The software has adopted the aluminum (Al) parameter values of electric conductivity $\sigma = 3.56 \times 10^7$ S/m, Rho (ρ) = 2700 kg/m^3, thermal conductivity (K) = 237 (W/K/m) in the range 150–2900 THz. These parameters are good agreement with the aluminum parameters of previously reported papers (Rakic et al. 1995, Palik 1998; Hossain et al. 2019b). We have considered the range of the proposed absorber from 375 to 750 nm. In the proposed structure,

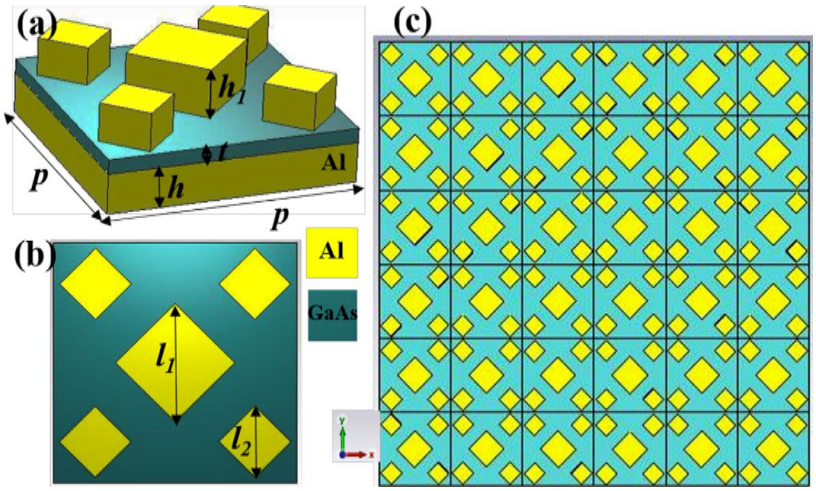

Fig. 1 **a** Schematic diagram of the MPA. **b** Program view. **c** Perspective view of a unit cell with the periodic range

Table 1 Respective parameter (nm) of the proposed MPA

Parameter	p	h	t	h_1	l_1	l_2
Value (nm)	610	100	37	100	150	90

we have considered the bottom layer to be a metallic aluminum plate with thickness greater than its skin depth for the operating frequency to eliminate the transmission losses. The semiconductor material of GaAs has some vital advantages such as high efficiency, high electron mobility and velocity, low-temperature coefficient, low light performance, and flexibility, etc. It has a direct bandgap that formation a good solar energy absorber. The description of GaAs are $\varepsilon = 12.94$, loss tangent (tanδ) = 0.006, ρ = 5320 (kg/m^3) and the thermal conductivity (K) = 54 (W/K/m) (Palik 1998; Hossain et al. 2019b). In the MPA structure, the periodic arrangement of the resonator at the top of the dielectric substrate plays a crucial role to gain a perfect absorber. Scattering parameters (S-parameter) are used for the absorption calculation of the proposed absorber. The condition of impedance matching is necessary to gain absorption because absorption depends on the impedance. The impedance of the proposed structure unit cell can be optimized by matching the impedance of metamaterial with free space impedance. By investigating the physical dimensions of the structure, the conditions of impedance matched with free space and the design structure give the near-unity absorption at an operating wavelength. Here, the impedance of design is very close to the impedance of free space, if these values are equal then the design absorber act as a super absorber.

In this work, we have chosen the CST microwave studio software for the simulation of the proposed structures. This software is a full-wave electromagnetic solver that uses the well-known theory FIT (Finite Integration Technique) to calculate the optical properties of the structures. So we have presented the absorption expression directly based on the scattering parameters. These scattering parameters can be used to evaluate the absorption (Mehrabi et al. 2018; Hossain et al. 2019a, b). The reflectance R(ω) and transmittance T(ω) depend on the scattering parameters such as $R(\omega) = |S_{11}|^2$ and $T(\omega) = |S_{21}|^2$. The scattering parameters S_{11} and S_{21} are described as

$$S_{11} = \sqrt{\frac{Reflected\ power\ form\ port1}{Incident\ power\ from\ port1}} \tag{1}$$

$$S_{21} = \sqrt{\frac{Transmitted\ power\ form\ port2}{Incident\ power\ from\ port1}} \tag{2}$$

The optical absorption properties of the proposed MPA in terms of frequency can be calculated by using the well-known equation expressed as,

$$\mathrm{A}(\omega) = 1 - \mathrm{R}(\omega) - \mathrm{T}(\omega) \tag{3}$$

where A(ω) and ω represent the absorption and angular frequency, respectively. In the proposed MPA, the thickness of the bottom aluminum layer is considered more than the skin depth, so it works as a reflector in the optical region so that the transmitted waves cannot pass through the structure. The absorber system contains two interfaces. One is the resonators layer, and the other is the ground film of Al metal. These layers act as a reflection/transmission surface that can reflect/transmit a part of the incident wave. If the considered ground layer works as a perfect reflector, the second-order reflection coefficient would be approx − 1, the transmission through the absorber will be approximately zero. Therefore, transmission becomes approximately zero in the above equation. Therefore, Eq. (3) can be written as;

$$\mathrm{A}(\omega) = 1 - R(\omega) = 1 - \left|S_{11}\right|^2 \tag{4}$$

To gain the efficient absorption level from scattering parameters, we applied the periodic boundary conditions for the proposed metamaterial structure. The unit cell periodic boundary conditions (PBCs) have been applied to the x and y-plane and the open-source was set in the z-direction (Floquet port) with a Perfect matched layer, respectively. All the axis are perpendicular to each other in the simulation setup (Mulla et al. 2016).

3 Results and discussion

Solar radiation covers the near-infrared to ultraviolet (100 to 1000 THz) frequency region but our work is in the visible region because it is widely used for various applications. To observe the optical performance of the proposed structure, we have used Eq. (4) to calculate the absorption and reflection of the absorber as shown in Fig. 2. Figure 2a manifested the absorption characteristics for the MPA with Al metal as the resonators and GaAs as a dielectric spacer layer. This design exhibits excellent broadband absorption in the optical region. We observe approx 100% broadband absorption from 591.54 to 704.40 nm (112.86 nm bandwidth) and an almost unity peak at 385.33 nm with 94.16%. In the broadband absorption region, we observe the three highest absorption peaks. These absorption peaks have 99.82%, 99.94%, and 99.94% absorption coefficients for the different wavelengths as 603.44 nm, 651.72 nm, and 692.05 nm, respectively. The comparison of the proposed MPA with literature work is presented in Table 2. When the electromagnetic wave strikes the absorber, some of the incident light is reflected in the free space which coefficient is S_{11} while some of the incident light is transmitted by region 1 to region 2 which coefficient is S_{21}. Here S_{11} and S_{21} represent the reflection and transmission coefficients,

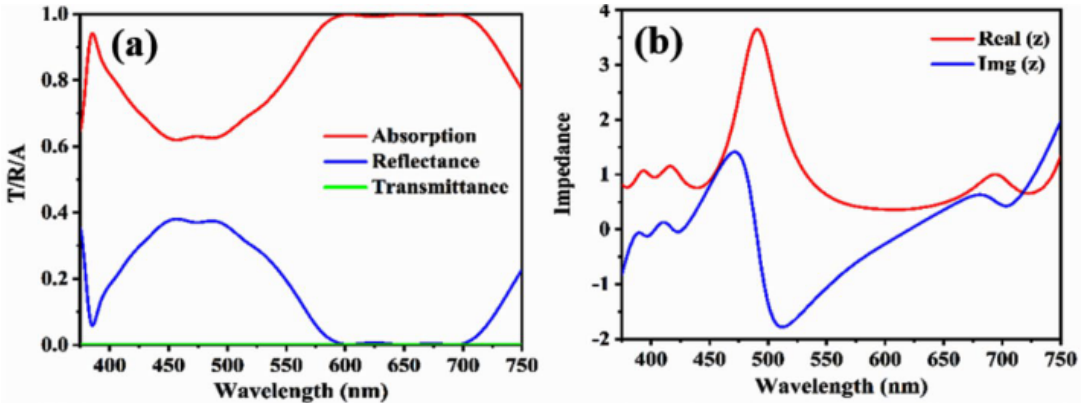

Fig. 2 **a** Absorption, reflectance, and transmittance spectra, and **b** the real and imaginary impedance of the proposed structure

Table 2 Comparative study of the proposed MPA with previously reported research papers

References	Dimensions of a unit cell	Dielectric thickness (nm)	Functionality	Absorptivity (%)
Rufangura and Sabah (2016a, b)	550×550	100	Single band	99.7
Rufangura and Sabah (2015)	600×600	93.5	Dual band	99.96, 99.37
Mulla and et al. (2016)	400×400	50	Multiband	99.2, 99.8, 99.9
Khan et al. (2018a, b)	400×300	80	Multiband	Above 90
Rufangura and Sabah (2018)	580×580	111.6	Multiband	99.95
Wu et al. (2020)	1000×1000	100	Multiband	99.9
This work	610×610	37	Wideband	>99, 94.16

respectively. Figure 2b exhibits the real and imaginary parts of impedance. Here transmittance power is zero ($|S_{21}|=0$) because the bottom layer of Al can not pass the light due to skin depth. We observe that the real and imaginary impedances at the unity absorption wavelength (385.33 nm, 603.44 nm, 651.72 nm, and 692.05) are close to near unity and zero, respectively. The effective impedance of the absorber is calculated by the scattering coefficients using the standard equation,

$$Z_{eff} = \sqrt{\frac{\left(1+S_{11}\right)^2 - S_{21}^2}{\left(1-S_{11}\right)^2 - S_{21}^2}} = \frac{1+S_{11}}{1-S_{11}} \tag{5}$$

The constitutive electromagnetic parameters such as effective permeability (μ_{eff}) and permittivity (ε_{eff}) can be calculated by the co-polarized reflection coefficient. The magnetic susceptibility (χ_{ms}) and electric susceptibility (χ_{es}) are help to evaluated (μ_{eff}) and (ε_{eff}) with distance (d) to be traveled by propagating wave, where $k_0=2\pi f/c$ is the wavenumber of the free space. We observe the negative values for the real part of permittivity and permeability within some specific wavelength regions from the results as shown in the

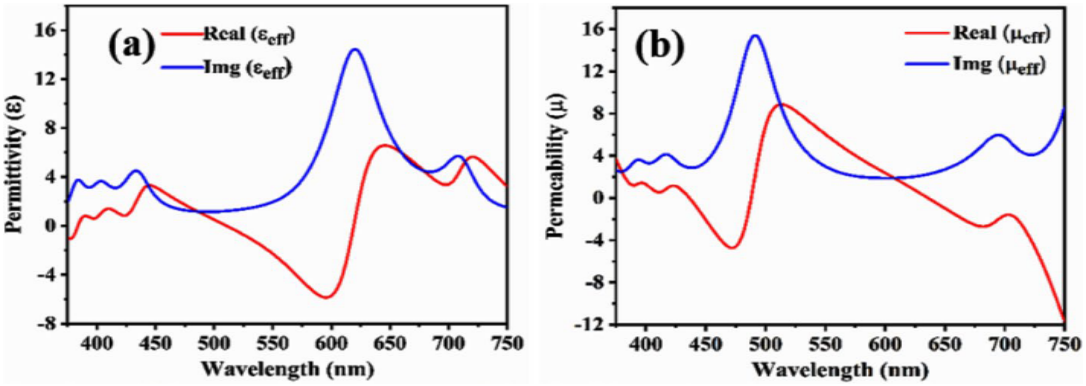

Fig. 3 The variations of the real and imaginary parts of the effective: **a** permittivity and **b** permeability

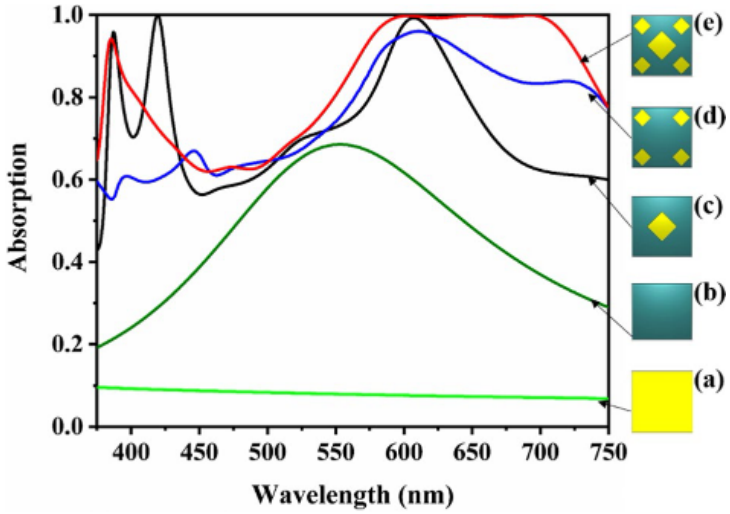

Fig. 4 Absorption variations with frequency for the structure with **a** Al substrate only, **b** Al-GaAs system **c** with only center resonator, **d** with corner resonators, **e** with corner and center resonators (complete unit cell)

figure. The variations of the real and imaginary parts of the effective permeability (μ_{eff}) and permittivity (ε_{eff}) are shown in Fig. 3. The expressions of the electric susceptibility (χ_{es}), magnetic susceptibility (χ_{ms}), effective permittivity (ε_{eff}) and permeability (μ_{eff}) are given below as (Yadav et al. 2018),

$$\begin{aligned} \chi_{es} &= 2j/k_0 * \left(1 - S_{11}/1 + S_{11}\right), \\ \varepsilon_{eff} &= 1 + \chi_{es}/d \end{aligned} \tag{6}$$

$$\begin{aligned} \chi_{ms} &= 2j/k_0 * \left(1 + S_{11}/1 - S_{11}\right) \\ \mu_{eff} &= 1 + \chi_{ms}/d \end{aligned} \tag{7}$$

To demonstrate the absorption responses for different cases, we have demonstrated the absorption, transmission and reflection responses for Al substrate only, substrate Al–GaAs layer and substrate Al–GaAs–Al resonators system in Fig. 4. We observe the maximum reflection, zero transmission, and approximately 8% average light absorption from the Al substrate as design (a). The absorption response exhibits around 45% absorbance for the structure of the Al-GaAs layer, as seen for design (b). These results are due to the

interaction between the absorbing and bottom layers. Maximum absorption is approximately 68.55% at the wavelength of 553.12 nm. When the inner resonator is established at the center of the dielectric spacer layer as design (c), the interaction of the resonator with the dielectric spacer layer and the bottom layer is formed three absorption peaks, as can be seen in the diagram. We obtain a perfect absorption of more than 99% absorption value at the resonance wavelengths 387.13 nm, 419.41 nm, and 607.35 nm. The response for the structure with corner resonators as design (d) is marked as a bold blue curve which gives a broader absorption response compared to the previous absorption level. This response gives the interaction between the corner resonator pairs and the other part of the structure with the help of electromagnetic responses. Finally, we have depicted the absorption responses for the combined resonators in one unit-cell as design (e) in Fig. 4 with a bold red curve. The interactions between the resonator and the coupling of Al-GaAs create the plasmonic effects, which are responsible for increasing the strength of the absorption. These results reveal the multiband topology for different structural arrangements. The significant absorption is the result of stimulated absorption in material GaAs due to Al material as a resonator and substrate layer with maximum reflection. The uses of Al materials as the resonators and reflector layer only trigger the efficient absorption in absorbing material because Al materials have a minimal absorption value. This result is due to the coupling of reflection and transmission and the plasmonic resonances effects of resonators and reflector layer.

To understand the absorption characteristics, it is necessary to know the impact of the geometric parameters. For the absorption mechanism, the parameters of dielectric layer thickness t, resonator diagonal lengths l_1, and l_2, and the structural periodicity p perform a very important role in the variation of absorption spectra. Firstly, we examine the effect of the dielectric layer thickness represented by the parameter t. The thickness of the dielectric layer can modulate the resonant wavelength and rate of absorption as shown in Fig. 5a. It mainly helps to the coupling between the resonators and the ground aluminum layer. Therefore, the magnetic response is generated by this coupling. Thus, the impedance matching of the absorber with the free space impedance verifies the electric and magnetic distribution. So, the thickness of dielectric separation generates the magnetic response when the parameter 't' is smaller and higher than 37 nm. The impedance condition does not match for other thicknesses (t), so absorption spectra are changed. Therefore, thickness plays a crucial role in the considered design absorber. The variations of the absorption

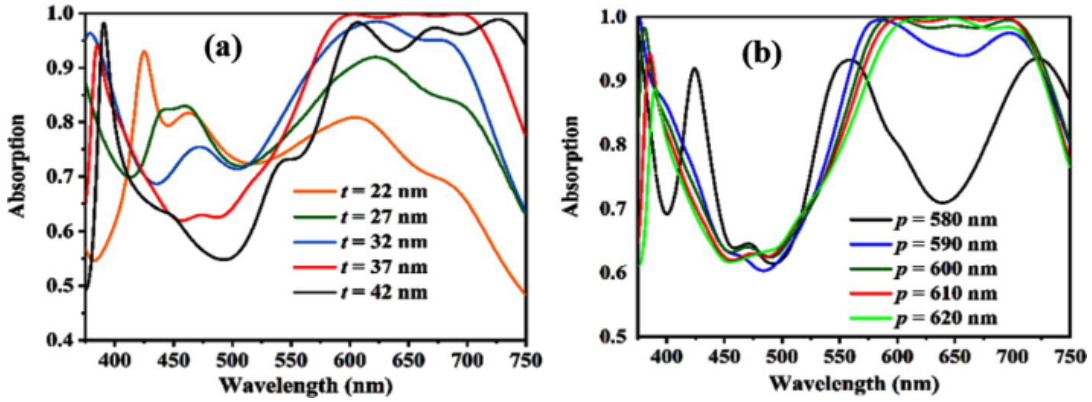

Fig. 5 Absorption spectra for different values of **a** dielectric layers thickness 't', and **b** periodicity parameter 'p'

with the periodicity of the unit cell 'p' are shown in Fig. 5b. When the period of a unit cell increases, the resonance peaks shift toward a higher wavelength with changed absorption values. It originates from the resonators because Electric-field and Magnetic-field are changing their positions. Therefore, we observe that the maximum absorptions are affected with changing of the periodicity and the optimized value is $p = 610$ nm to obtain the perfect absorption.

In the design of the absorber, the resonator's dimension selection also plays an important role in investigating the perfect absorption. Tuning the resonator's dimension influences the absorption spectrum with constant values of the other parameters. The results with different resonator dimensions are shown in Fig. 6. The red curve represents the desired results for perfect absorption. As seen in Fig. 6a, the absorption depends on the diagonal length of resonators so this section explained the optimization of the diagonal length l_1 of the middle resonator. The variations of the absorption with the diagonal length of the middle resonators are shown in Fig. 6b. The resonance wavelength 591.54 to 704.40 nm and 385.33 nm are strongly dependent on the diagonal length of resonators which give the transformation of electric and magnetic responses at this wavelength. This result is the interaction between resonators. Therefore, finding the perfect absorption requires adjusting the diagonal length 'l_1'. Similarly, we have investigated the absorption results with a different diagonal length of corner resonators at the same wavelength. The distributions of the absorption at the different values of diagonal length 'l_2' are shown in Fig. 6b. We obtain the best results with diagonal length $l_2 = 90$ nm as seen in Fig. 6b. Thus, the properties of the MPA can be modulated by adjusting the individual resonators or their grouping.

The directions of the solar radiation change every time in the sky and some parts of the incident radiation on the unit cell are in the form of unpolarised radiations. Thus, a convenient metamaterial unit cell design is required to operate for all the incident electromagnetic radiations for optimizing the absorption. The simulated absorption results for both modes at different polarisation angles are shown in Fig. 7a and b. It can be seen that the absorption spectra for different polarization angles (0°-90°) are the same within the operating wavelength because the proposed design is symmetrical. In the visible region, the polarization angle is very important for the design of a metamaterial absorber because efficient absorption is necessary for solar cells. The absorption spectra with various incident angles (θ) are shown in Fig. 7c and d to characterize the absorber performance at different incident angles (0°-50°) for TE and TM-modes.

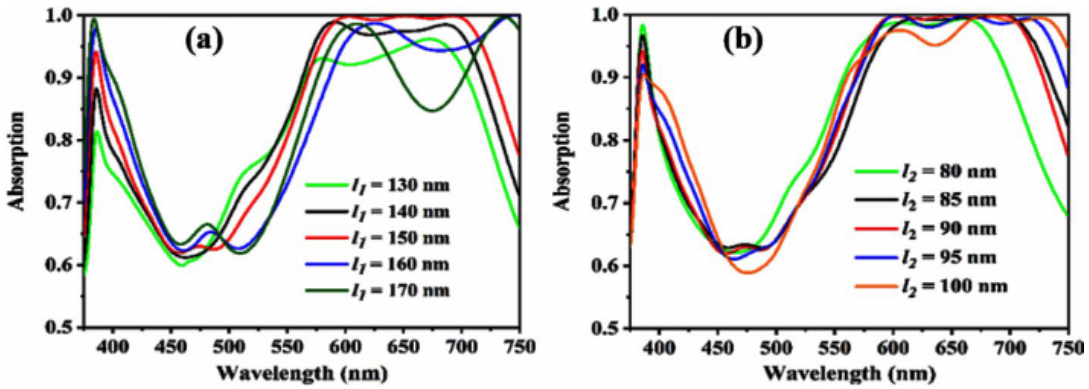

Fig. 6 Absorption spectra for various values of **a** the diagonal length 'l_1' of the middle resonator, **b** the diagonal length 'l_2' of the corner resonator

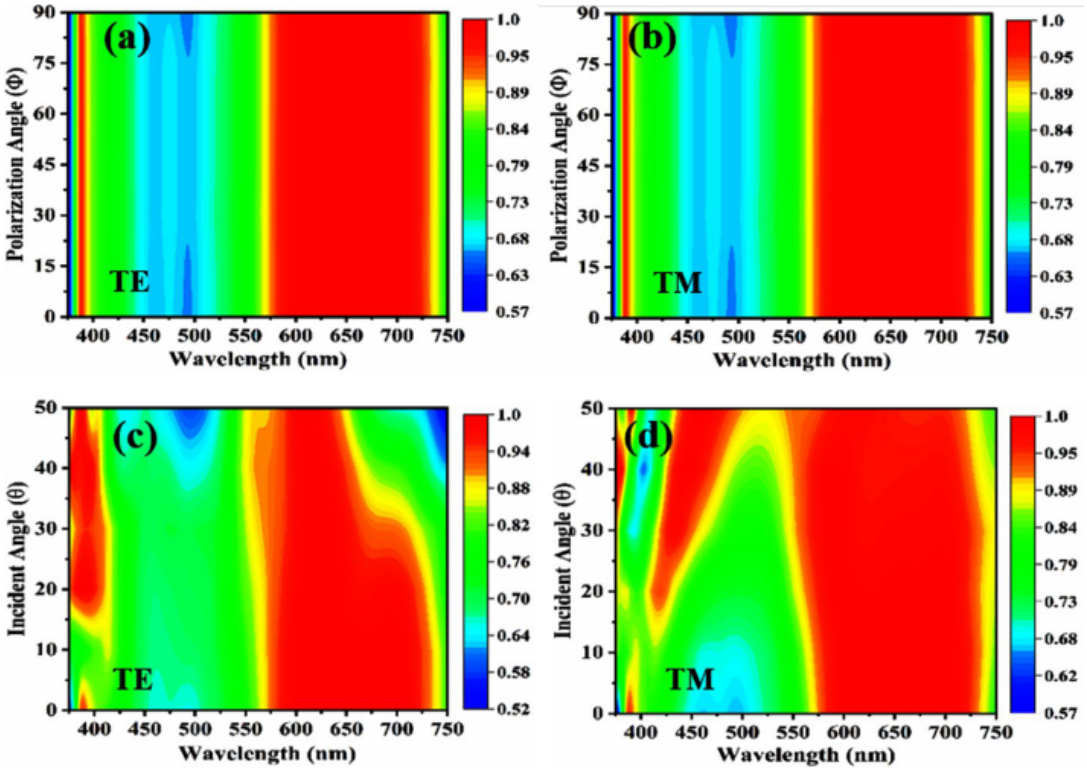

Fig. 7 **a**, **b** Absorption spectra for the different polarization angles (0°-90°), and **c**, **d** the different incident angles (0°-50°) with TE mode and mode

The absorption coefficients decrease with increasing the incident angles for TE mode as shown in Fig. 7c. The distributions of absorption with incident angle are mainly affecting within wavelength range 591.54 nm to 704.40 nm due to the electric and magnetic mode excitations. Figure 7d shows the absorption spectra for TM mode. In this case, we obtain the broadband absorption efficiency as compared to the TE mode's absorption and absorbance increases with the incident angles. The comparison of our results with the previously reported papers is tabulated in Table 2. The proposed absorber exhibits a good absorption level compared to the previously reported works in terms of their absorption coefficients, impedance, and production cost.

Nowadays, different materials are used for different layers to gain strong absorption. So, We have used different metals (Au, Ag, Cu, and Al) for resonators to investigate the performance of our proposed design absorber. Figure 8a shows the simulated absorption results with different resonator metals. As the result, we obtain the perfect absorption for the proposed absorber with Al over the whole optical region as can be seen in Fig. 8a. The selections of the resonator metals are very important because it reveals the coupling of surface plasmons which help to achieve strong absorption. Figure 8b demonstrated the absorption performance with various materials (silicon dioxide (SiO_2), silicon nitride (Si_3N_4), indium tin oxide (ITO), and gallium arsenide (GaAs)) of the dielectric spacer layers. The absorption changed with different bandwidths for each of the spacer materials, and GaAs show the strong and highest absorption coefficients as compared to other dielectric materials.

Various parameters of structure demonstrated different absorbances in the optical region. Here we evaluated the absorbance under the AM1.5 (air mass 1.5) solar spectrum ($A_{AM1.5}$) of the solar cell. The large conversion efficiency can be obtained when the value of $A_{AM1.5}$ is higher. To check the light trapping effect of the unit cell used the $A_{AM1.5}$ (Khan

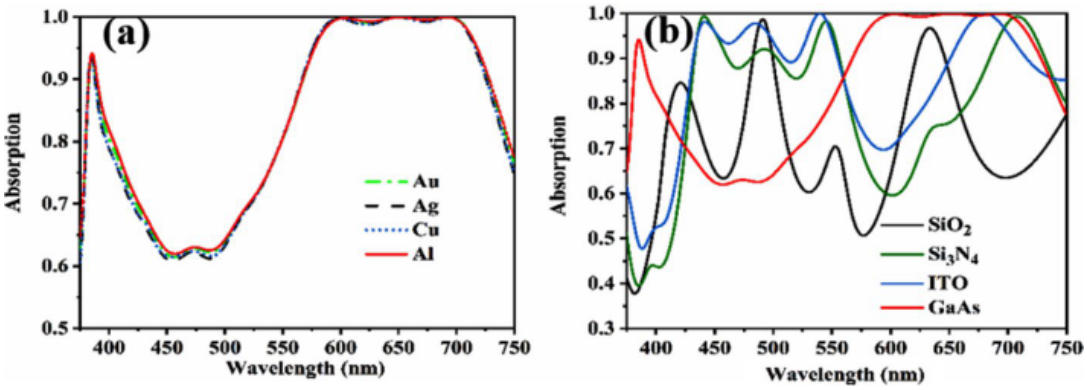

Fig. 8 **a** Absorption spectra for the different resonator metals such as Au Ag, Cu, and Al, and **b** absorption spectra for the dielectric spacer layer of SiO_2, Si_3N_4, ITO, and GaAs

et al. 2018a, b). In this context, the proposed absorber provides ultra-wideband absorption in the optical spectrum.

From this expression, we can obtain the $A_{AM1.5}$ of the solar cell,

$$A_{AM1.5} = \frac{\int_{\lambda 1}^{\lambda 2} A(\lambda)N(\lambda)d\lambda}{\int_{\lambda 1}^{\lambda 2} N(\lambda)d\lambda}, \tag{8}$$

where λ is the wavelength of light, λ_1, and λ_2 define the spectrum range of absorption, Thickness (λ) is the absorption of investigated structure, and $N(\lambda)=\frac{w(\lambda)}{E(\lambda)}$ is the photon numbers distribution under the AM1.5 solar illumination. Where w(λ) and E(λ) represent the solar spectral irradiance and energy of the photon. We evaluated the A(λ) and N(λ) using with below equation under the different geometrical parameters of structure as the dielectric thickness (t) and the dimension of the unit cell (p). Figure 9a and b shown the maximum $A_{AM1.5}$ is 85.78% for $t=37$ nm and 86.12% for $p=600$ nm. The value of conversion efficiency (represent $A_{AM1.5}$) of solar cells should be maximum.

In Fig. 10a, we investigated the short circuit current density (J_{sc}) with the thickness effect of the dielectric layer of GaAs. One electron–hole pair is generated by each absorbed photon

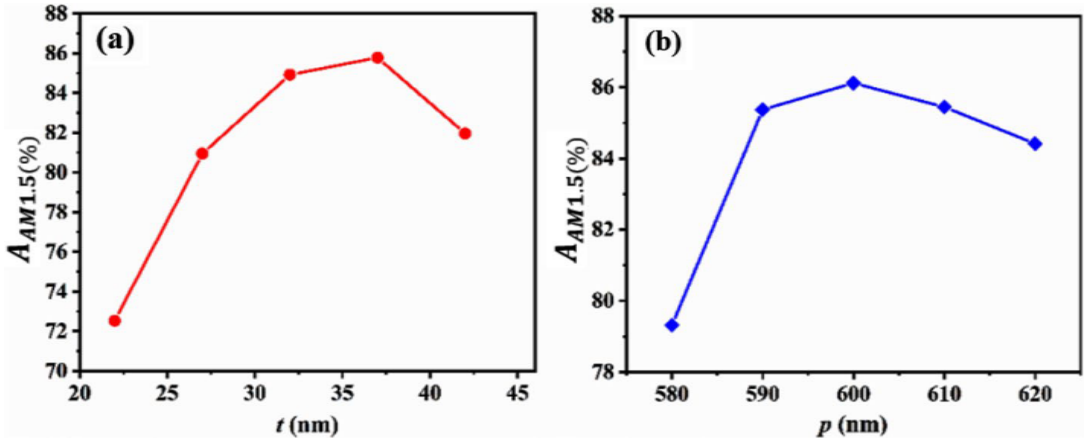

Fig. 9 The evaluated values of $A_{AM1.5}$ as a function of **a** dielectric thickness (t), and **b** unit cell dimension (p)

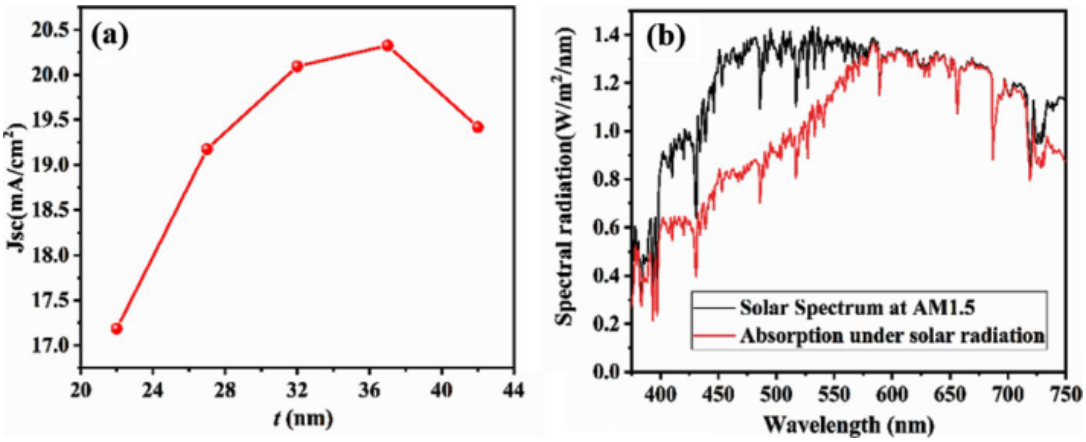

Fig. 10 **a** Short circuit current density (J_{sc}) with various thicknesses of GaAs layer, **b** Absorption diagram of absorber under the AM1.5 solar spectrum

and collected carriers are generated by all photons. J_{sc} under AM1.5 solar irradiance can be calculated by this expression,

$$J_{sc} = \frac{q}{hc} \int_{\lambda 1}^{\lambda 2} \lambda \Phi_{AM1.5} A(\lambda) d\lambda \tag{9}$$

here q is the charge of an electron, λ is the wavelength of the incident light, c is the speed of light, h is the Plank constant, A(λ) is the absorption of this absorber, $\Phi_{AM1.5}$ is the solar radiance, and considering the quantum efficiency (internal) is 100%. When the GaAs thickness is tuned from 22 to 42 nm with an interval of 5 nm, J_{sc} is not regular because J_{sc} mainly depends on the number of resonant modes generated in the 375–750 nm wavelength range as shown in Table 3. The maximum J_{sc} obtained for t = 32 nm, which is 20.10 mA/cm^2, for t = 37 nm, J_{sc} = 20.33 mA/cm^2, which is greater than the, J_{sc} of 17.08 mA/cm^2, 13.2 mA/cm^2, 14.09 mA/cm^2 reported paper (Li et al. 2020, Wu et al. 2018, Wang et al. 2015). From the response of solar absorption, can find the solar energy collection. The ideal absorber has > 99% absorbance in the operating region and shows a wide bandwidth. We investigated the solar absorption of the proposed absorber under the irradiance of the AM1.5 source. In Fig. 10b, somewhere energy is missed, but somewhere energy is matched under the illumination there efficiency is high of capture light. Therefore, this absorber can be used the solar cell and solar energy harvesting-related potential applications.

4 Conclusions

In this study, we have presented a polarization-insensitive-based metamaterial absorber structure that exhibited a near-unity absorption from 591.54 to 704.40 nm due to impedance matching conditions. The proposed structure has been designed with three effective layers

Table 3 J_{sc} with different thickness (t) of a dielectric layer,

Thickness (t)	22 nm	27 nm	32 nm	37 nm	42 nm
J_{sc}(mA/cm^2)	17.18	19.17	20.10	20.33	19.42

arrangement (metal-dielectric-metal). The position and amplitude of absorption bands can be tuned with the parameters of resonators and thickness of the constituted dielectric layer. The effects of polarization angles and incident angles on the absorption of the design have also been demonstrated. The large value of $A_{AM1.5}$ indicates improved conversion efficiency and promising for solar cell applications. This absorber can be applied in electricity because it has a high short circuit current density of over 20.33 mA/cm^2. Moreover, the proposed multiband absorber can be used to design optical detectors, sensors, optical imaging, and solar energy harvesting devices.

Acknowledgements One of the authors (Raj Kumar) is thankful to The University Grants Commission (UGC), India for providing the senior research fellowship. Bipin K. Singh is thankful to The University Grants Commission (UGC), India, for providing financial support in the form of Dr. D. S. Kothari Postdoctoral Fellowship.

References

Almoneef, T.S., Ramahi, O.M.: Metamaterial electromagnetic energy harvester with near unity efficiency. Appl. Phys. Lett. **106**(15), 153902 (2015)

Aydin, K., Ferry, V.E., Briggs, R.M., Atwater, H.A.: Broadband polarization-independent resonant light absorption using ultrathin plasmonic super absorbers. Nat. Commun. **2**(1), 1–7 (2011)

Boriskina, S.V., Ghasemi, H., Chen, G.: Plasmonic materials for energy: From physics to applications. Mater. Today **16**(10), 375–386 (2013)

Cheng, Y., Du, C.: Broadband plasmonic absorber based on all silicon nanostructure resonators in visible region. Opt. Mater. **98**, 109441 (2019)

Dayal, G., Ramakrishna, S.A.: Design of multi-band metamaterial perfect absorbers with stacked metal-dielectric disks. J. Opt. **15**(5), 055106 (2013)

Ding, F., Jin, Y., Li, B., Cheng, H., Mo, L., He, S.: Ultrabroadband strong light absorption based on thin multilayered metamaterials. Laser Photon. Rev. **8**(6), 946–953 (2014)

Ding, C., Jiang, L., Wu, L., Gao, R., Xu, D., Zhang, G., Yao, J.: Dual-band ultrasensitive THz sensing utilizing high quality Fano and quadrupole resonances in metamaterials. Opt. Commun. **350**, 103–107 (2015)

Gao, H., Peng, W., Liang, Y., Chu, S., Yu, L., Liu, Z., Zhang, Y.: Plasmonic broadband perfect absorber for visible light solar cells application. Plasmonics **15**(2), 573–580 (2020)

Hasan, M., Rahman, M., Faruque, M.R.I., Islam, M.T., Khandaker, M.U.: Electrically compact SRR-loaded metamaterial inspired quad-band antenna for Bluetooth/WiFi/WLAN/WiMAX system. Electronics **8**(7), 790 (2019)

He, X., Yan, S., Lu, G., Zhang, Q., Wu, F., Jiang, J.: An ultra-broadband polarization-independent perfect absorber for the solar spectrum. RSC Adv. **5**(76), 61955–61959 (2015)

Hossain, M.J., Faruque, M.R.I., Ahmed, M.R., Alam, M.J., Islam, M.T.: Polarization-insensitive infrared-visible perfect metamaterial absorber and permittivity sensor. Results Phys. **14**, 102429 (2019a)

Hossain, M.J., Faruque, M.R.I., Islam, M.T.: Correction: perfect metamaterial absorber with high fractional bandwidth for solar energy harvesting. PLoS ONE **14**(1), e0211751 (2019b)

Khan, A.D., Khan, A.D., Khan, S.D., Noman, M.: Light absorption enhancement in tri-layered composite metasurface absorber for solar cell applications. Opt. Mater. **84**, 195–198 (2018a)

Khan, A.D., Iqbal, J., ur Rehman, S.: Polarization-sensitive perfect plasmonic absorber for thin-film solar cell application. Appl. Phys. A **124**(9), 1–9 (2018)

Kumar, R., Singh, B.K., Pandey, P.C.: Study of gallium arsenide based perfect metamaterial absorber in the broadband region. In: IEEE 17th India Council International Conference (INDICON), pp. 1–4 (2020)

Landy, N.I., Sajuyigbe, S., Mock, J.J., Smith, D.R., Padilla, W.J.: Perfect metamaterial absorber. Phys. Rev. Lett. **100**(20), 207402 (2008)

Li, C., Xiao, Z., Ling, X., Zheng, X.: Broadband visible metamaterial absorber based on a three-dimensional structure. Waves Random Complex Media **29**(3), 403–412 (2019)

Li, H., Hu, Y., Yang, Y., Zhu, Y.: Theoretical investigation of broadband absorption enhancement in a-Si thin-film solar cell with nanoparticles. Sol. Energy Mater. Sol. Cells **211**, 110529 (2020)

Liu, N., Mesch, M., Weiss, T., Hentschel, M., Giessen, H.: Infrared perfect absorber and its application as plasmonic sensor. Nano Lett. **10**(7), 2342–2348 (2010)
Liu, K., Jiang, S., Ji, D., Zeng, X., Zhang, N., Song, H., Xu, Y., Gan, Q.: Super absorbing ultraviolet metasurface. IEEE Photon. Technol. Lett. **27**(14), 1539–1542 (2015)
Mahmud, M., Islam, M.T., Misran, N., Singh, M.J., Mat, K.: A negative index metamaterial to enhance the performance of miniaturized UWB antenna for microwave imaging applications. Appl. Sci. **7**(11), 1149 (2017)
Mahmud, S., Islam, S.S., Mat, K., Chowdhury, M.E., Rmili, H., Islam, M.T.: Design and parametric analysis of a wide-angle polarization-insensitive metamaterial absorber with a star shape resonator for optical wavelength applications. Results Phys. **18**, 103259 (2020)
Maier, T., Brueckl, H.: Multispectral microbolometers for the midinfrared. Opt. Lett. **35**(22), 3766–3768 (2010)
Mehrabi, M., Rajabalipanah, H., Abdolali, A., Tayarani, M.: Polarization-insensitive, ultra-broadband, and compact metamaterial-inspired optical absorber via wide-angle and highly efficient performances. Appl. Opt. **57**(14), 3693–3703 (2018)
Melik, R., Unal, E., Perkgoz, N.K., Puttlitz, C., Demir, H.V.: Metamaterial-based wireless strain sensors. Appl. Phys. Lett. **95**(1), 011106 (2009)
Mulla, B., Sabah, C.: Perfect metamaterial absorber design for solar cell applications. Waves Random Complex Media **25**(3), 382–392 (2015)
Mulla, B., Sabah, C.: Multi-band metamaterial absorber design based on plasmonic resonances for solar energy harvesting. Plasmonics **11**(5), 1313–1321 (2016)
Mulla, B., Sabah, C.: Multi-band metamaterial absorber topology for infrared frequency regime. Physica E **86**, 44–51 (2017)
Palik, E.D.: Handbook of Optical Constants of Solids, vol. 3. Academic Press, New York (1998)
Rakic, A.D.: Algorithm for the determination of intrinsic optical constants of metal films: application to aluminium. Appl. Opt. **34**(22), 4755–4767 (1995)
Rakic, A.D., Djurisic, A.B., Elazar, J.M., Majewski, M.L.: Optical properties of metallic films for vertical-cavity optoelectronic devices. Appl. Opt. **37**(22), 5271–5283 (1998)
Rufangura, P., Sabah, C.: Polarization angle insensitive dual-band perfect metamaterial absorber for solar cell applications. Phys. Status Solidi C **12**(911), 1241–1245 (2015)
Rufangura, P., Sabah, C.: Polarisation insensitive tunable metamaterial perfect absorber for solar cells applications. IET Optoelectron. **10**(6), 211–216 (2016a)
Rufangura, P., Sabah, C.: Wide-band polarization-independent perfect metamaterial absorber based on concentric rings topology for solar cells application. J. Alloy Compd. **680**, 473–479 (2016b)
Rufangura, P., Sabah, C.: Graphene-based wideband metamaterial absorber for solar cells application. J. Nanophotonics **11**(3), 036008 (2017)
Rufangura, P., Sabah, C.: Perfect metamaterial absorber for applications in sustainable and high-efficiency solar cells. J. Nanophoton. **12**(2), 026002 (2018)
Shalaev, V.M., Cai, W., Chettiar, U.K., Yuan, H.K., Sarychev, A.K., Drachev, V.P., Kildishev, A.V.: Negative index of refraction in optical metamaterials. Opt. Lett. **30**(24), 3356–3358 (2005)
Shemelya, C., DeMeo, D., Latham, N.P., Wu, X., Bingham, C., Padilla, W., Vandervelde, T.E.: Stable high temperature metamaterial emitters for thermophotovoltaic applications. Appl. Phys. Lett. **104**(20), 201113 (2014)
Shoshi, A., Brückl, H., Reichl, W., Niessner, G., Maier, T.: B4. 1-wavelength-selective metamaterial absorber for thermal detectors. In: Proceedings SENSOR 2015, pp. 251–256 (2015).
Smith, D.R., Padilla, W.J., Vier, D.C., Nemat-Nasser, S.C., Schultz, S.: Composite medium with simultaneously negative permeability and permittivity. Phys. Rev. Lett. **84**(18), 4184 (2000)
Wang, H., Wang, L.: Plasmonic light trapping in an ultrathin photovoltaic layer with film-coupled metamaterial structures. AIP Adv. **5**(2), 027104 (2015)
Wu, C., Neuner, B., III., John, J., Milder, A., Zollars, B., Savoy, S., Shvets, G.: Metamaterial-based integrated plasmonic absorber/emitter for solar thermo-photovoltaic systems. J. Opt. **14**(2), 024005 (2012)
Wu, S., Ye, Y., Luo, M., Chen, L.: Ultrathin omnidirectional, broadband visible absorbers. JOSA B **35**(8), 1825–1828 (2018)
Wu, P., Zhang, C., Tang, Y., Liu, B., Lv, L.: A perfect absorber based on similar Fabry-Perot four-band in the visible range. Nanomaterials **10**(3), 488 (2020)
Yadav, V.S., Ghosh, S.K., Bhattacharyya, S., Das, S.: Graphene-based metasurface for a tunable broadband terahertz cross-polarization converter over a wide angle of incidence. Appl. Opt. **57**(29), 8720–8726 (2018)

Yin, X., Long, C., Li, J., Zhu, H., Chen, L., Guan, J., Li, X.: Ultra-wideband microwave absorber by connecting multiple absorption bands of two different-sized hyperbolic metamaterial waveguide arrays. Sci. Rep. **5**(1), 1–8 (2015a)

Yin, X., Chen, L., Li, X.: Ultra-broadband super light absorber based on multi-sized tapered hyperbolic metamaterial waveguide arrays. J. Lightwave Technol. **33**(17), 3704–10 (2015b)